

Magnetic resonance in the ordered phases of the 2D frustrated quantum magnet Cs_2CuCl_4

A. I. Smirnov,^{1,2} K. Yu. Povarov,¹ S. V. Petrov,¹ and A. Ya. Shapiro³

¹*P. L. Kapitza Institute for Physical Problems, RAS, 119334 Moscow, Russia*

²*Moscow Institute for Physics and Technology, 141700, Dolgoprudny, Russia*

³*A. V. Shubnikov Institute of Crystallography, RAS, 119333 Moscow, Russia*

(Dated: February 6, 2012)

The temperature evolution of the electron spin resonance is studied at cooling the crystal samples of Cs_2CuCl_4 through the Néel point 0.62 K. A coexistence of the high-frequency spinon type resonance developed in the spin-liquid phase and of the low-frequency antiferromagnetic resonance was found in the ordered phase. The low-frequency magnetic resonance spectrum in the low field range has two gapped branches and corresponds well to the spectrum of spin excitations of a planar spiral spin structure with two axes of the anisotropy. The field induced phase transitions result in a more complicated low-frequency spectra.

PACS numbers: 76.30.-v, 75.40.Gb, 75.10.Jm

INTRODUCTION

Magnetic crystals with low dimensional and frustrated antiferromagnetic exchange interaction remain in a correlated paramagnetic state (often called "spin liquid phase") far below the Curie-Weiss temperature T_{CW} . The suppression or even absence of the ordering is due to strong quantum fluctuations. A quasi 2D $S = 1/2$ dielectric antiferromagnet Cs_2CuCl_4 is a thoroughly studied example of a magnetic system with spin correlations emergent in a wide temperature range below $T_{CW}=4$ K, but still above the ordering point $T_N=0.62$ K. In crystals of Cs_2CuCl_4 the Cu^{2+} magnetic ions are placed on stacked 2D layers with distorted triangular lattice. Experiments on inelastic neutron scattering in the spin-liquid phase uncovered magnetic excitations propagating along b -axis with a spectrum of an extensive multiparticle continuum [1, 2]. The wide band of transferred energy corresponding to a fixed transferred momentum q is observed for $q \sim \frac{1}{b}$, where b is a lattice period, while at low momenta $q \ll \frac{1}{b}$ the spectrum width is negligible in zero magnetic field. The boundaries and the spectral density of the continuum observed in Cs_2CuCl_4 correspond well to the two-spinon continuum of a quantum critical spin $S=1/2$ chain [1, 3]. The 1D nature of spinon excitations in this 2D structure is attributed to the frustration of exchange bonds on the distorted triangular lattice, with the strong exchange bonds ($J=0.375$ meV) directed along b -direction, and a weaker exchange interaction ($J' = 0.34J$), coupling magnetic Cu^{2+} ions along lateral sides of isosceles triangles, see Fig. 1. The interlayer exchange $J''=0.045J$ is the weakest one. The spin chains extended along b -direction should be practically decoupled from each other due to the geometric frustration of the exchange bonds J' , as shown in numerical simulations [4] and in the analytical approach [3]. Another consequence of the frustration is the extreme sensitivity of the ground state to the weak interlayer ex-

change and Dzyaloshinsky-Moriya interaction [5]. The study of elastic neutron scattering [1] showed, that the ordering at T_N results in a spiral spin structure. The spiral lies approximately in the bc -plane and its wavevector is directed along b -axes. The ordered spin component has a strong quantum reduction $\Delta S/S=0.25$ [6].

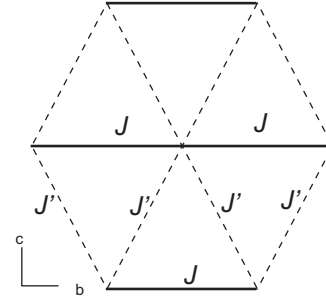


FIG. 1. Sketch of the exchange paths of Cs_2CuCl_4 within the bc -plane

The spinon continuum in Cs_2CuCl_4 corresponds mainly to that of $S=1/2$ Heisenberg antiferromagnetic chain. Nevertheless, it is modified in the low-frequency range by the uniform Dzyaloshinsky-Moriya interaction of magnetic ions within a chain [7–9]. The uniform Dzyaloshinsky-Moriya interaction between the spins in a chain is a distinct feature of Cs_2CuCl_4 . The corresponding model Hamiltonian is derived in Ref. [5], it's terms D_a and D_c present this interaction. Besides, the Dzyaloshinsky-Moriya interaction of a conventional, i.e. staggered, type is present for the ions connected by exchange bonds J' . This interaction corresponds to terms D'_a and D'_c of the Hamiltonian of Ref. [5]. The uniform interaction results in the shift of the continuum spectrum $E(q)$ along the q axis for a value of $\delta q = \sqrt{D_a^2 + D_c^2}/(Jb)$. A zero field gap arises due to this shift. The shift results also in an essential change of the envelope of the spectrum of spin fluctuations at $q=0$ in a magnetic field aligned par-

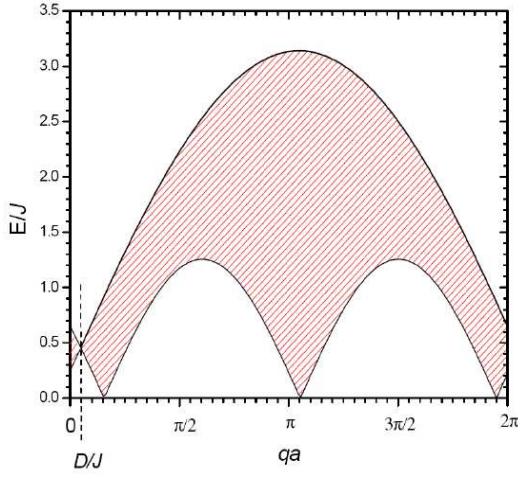


FIG. 2. The continuum of transversal spin excitations for 1D spin chain with the uniform Dzyaloshinsky-Moriya interaction in a magnetic field $H = 0.5J/(g\mu_B)$ at $\mathbf{H} \parallel \mathbf{D}$. Note a considerable width of the continuum at $q=0$.

allel to the Dzyaloshinsky-Moriya vector $\mathbf{D} = (D_a, D_c)$. The $q = 0$ spectrum, which in the absence of uniform Dzyaloshinsky-Moriya interaction is represented by a single Zeeman frequency $\mu_B H/\hbar$, transforms in a band of frequencies corresponding to the width of the continuum, $\sim J\delta q$, see Fig. 2. This results in an effective splitting of the electron spin resonance (ESR) line at $\mathbf{H} \parallel \mathbf{D}$, because the spectral density has singularities at the boundaries of the continuum [7]. For $\mathbf{H} \perp \mathbf{D}$, there is no splitting, while the gap in the ESR spectrum causes an essential shift of the ESR line. The zero-field gap in the ESR spectrum, shift of the resonance field at $\mathbf{H} \parallel b$ and split doublet at $\mathbf{H} \perp b$, in accordance with vector \mathbf{D} orientation in Cs_2CuCl_4 were indeed observed [8] in the temperature range of the spin-liquid phase. The gap at $T = 2T_N = 1.3$ K has a value of 14 GHz, about a half of the zero-temperature gap in the ordered phase.

The aim of the present work is to study the temperature evolution of the above exotic spinon-type ESR (with the gap opening above T_N and anisotropic splitting) at cooling through T_N , as well as the study of the antiferromagnetic resonance at low temperatures. We observe a surprising ESR spectrum at low temperatures: for the higher frequency band, above 60 GHz, the spinon-type doublet ESR was observed to be preserved till the lowest temperature, while for low frequencies, below 40 GHz the spinon magnetic resonance is replaced by the antiferromagnetic resonance. The coexistence of spinon resonance and antiferromagnetic resonance at low temperatures presents a new kind of ESR spectrum of a spin $S=1/2$ quantum antiferromagnet.

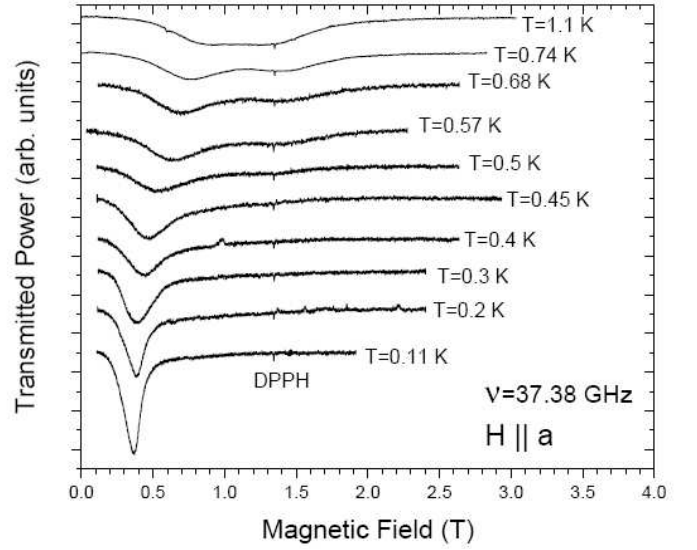


FIG. 3. Temperature evolution of the ESR signal in the low frequency range at $\mathbf{H} \parallel a$. Weak sharp resonances at $H=1.35$ T is a $g=2.0$ label of free radicals in diphenyl-picryl-hydrazil (DPPH).

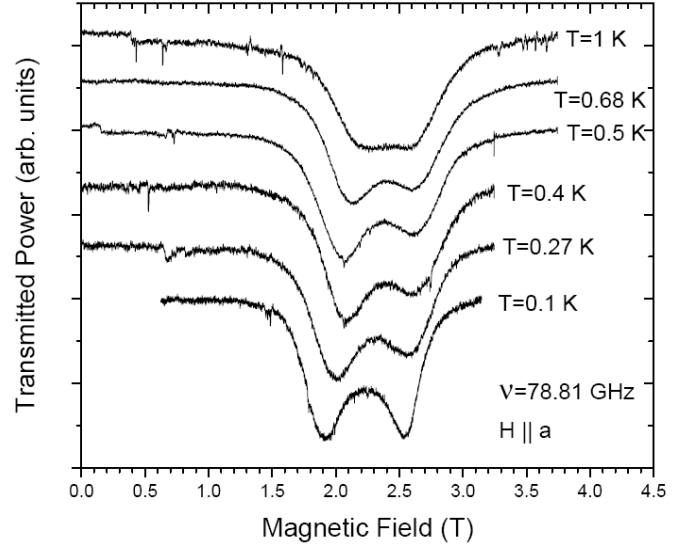


FIG. 4. Temperature evolution of the ESR signal in a high frequency range at $\mathbf{H} \parallel a$.

EXPERIMENT

The magnetic resonance signals were recorded as field dependences of the transmitted microwave power in the frequency range $25 < \nu < 140$ GHz, using multimode microwave resonator and waveguide insert combined with a dilution refrigerator Kelvinox-400. The sample was fixed by the Apeizon N grease inside the copper resonator, placed in vacuum and connected via a thermoconducting link to the mixing chamber of the dilution refrigerator. The temperature of the resonator was monitored

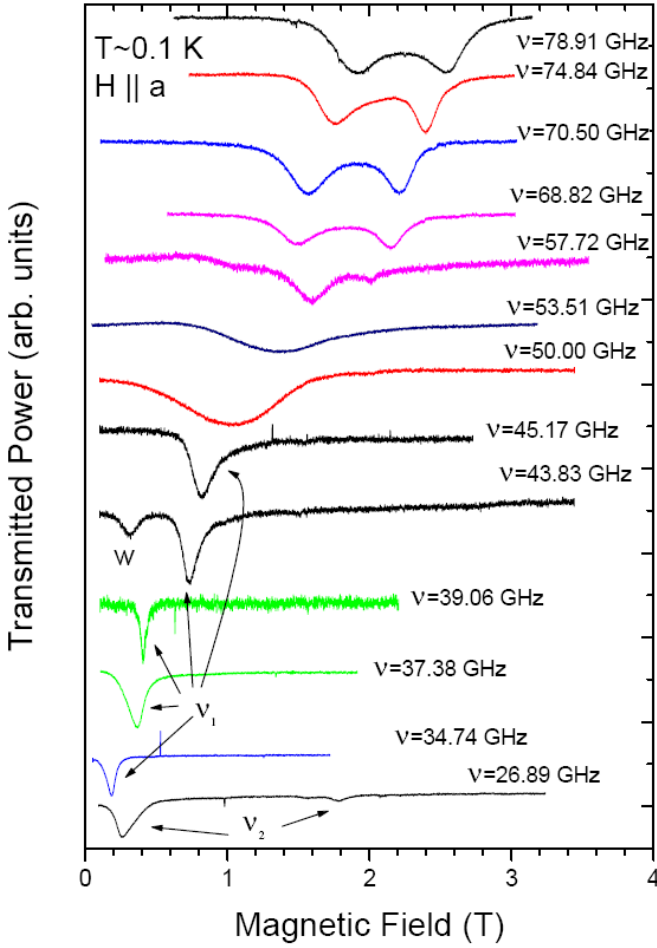


FIG. 5. ESR lines at $T < 0.1$ K and $\mathbf{H} \parallel a$ for different frequencies

by a RuO_2 thermometer placed on the top of the resonator. To avoid heating of the resonator unit during experiments at the temperatures below 1 K, the screening of the infrared thermal radiation, passing through the waveguides, was performed by two filters thermalized at 80 K and at 4 K, following Ref. [10]. The incident microwave power at the cryostat input was not higher than $1 \mu\text{W}$. Microwave absorption by the sample is estimated as 1 nW, for this estimation we used the measurements of the transmission of the waveguides with filters and of the coupling between the resonator and waveguides, as well as the typical ratio of microwave losses in the sample and in the resonator walls. The overheating of the sample due to microwave absorption is estimated as 10 mK at $T = 0.1$ K. Considering the above estimations we can not surely distinct the temperatures of the sample below 0.1 K, despite the observation that thermometer at the top of the resonator indicated temperature down to 0.05 K during the field sweep. We checked the sample heating effects by making experiments with different values of the incident microwave power. At enlarging the power we marked the power level causing overheating of the resonator or

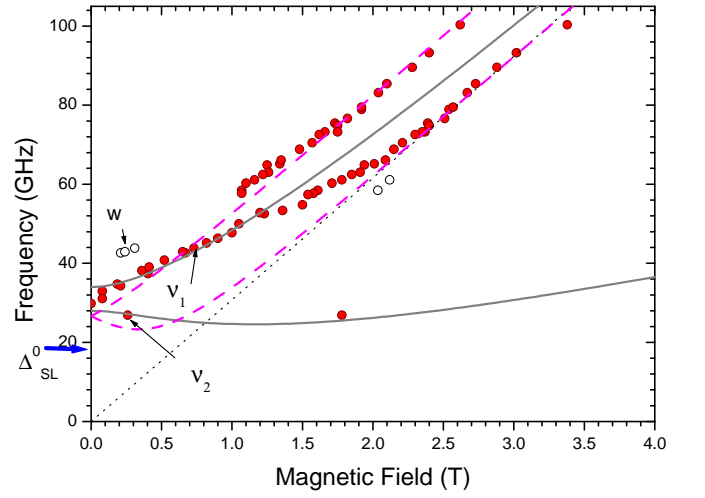


FIG. 6. Frequency-field dependence for ESR in Cs_2CuCl_4 at $T < 0.1$ K and $\mathbf{H} \parallel a$. Filled symbols correspond to the intensive ESR modes, empty symbols present resonances of a weak intensity. Solid lines correspond to the calculation according to eq. (8). Dashed lines present the proposed spinon-type resonances, ν_{\pm} , according to relation (3). Dotted line corresponds to the ESR of noninteracting spins with $g = g_a$.

change of the ESR lineshape or position. After that, an attenuation for more than a factor of 2 was inserted for the incident power. The samples from the same batch as in Ref. [8] were used. As reported in Ref. [8], the ESR signal at $T > 10$ K is a typical single mode resonance corresponding to g -factor values $g_{a,b,c} = 2.20, 2.08, 2.30$ for the orientation of the magnetic field along the crystallographic axes a, b and c correspondingly. At cooling below 4 K a significant change of ESR lineshape and position was found: for the temperature $T = 1.3$ K and $\mathbf{H} \parallel b$ the resonance line is shifted to lower fields, while for $\mathbf{H} \parallel a, c$ it is transformed to a doublet due to the modification of the spinon continuum described above. Now we describe the transformation of the ESR lines at further cooling through the ordering point $T_N = 0.62$ K.

Field along a -axis

At first, we consider the temperature evolution of ESR signals for the most simple case of $\mathbf{H} \parallel a$. Here the magnetic field is perpendicular to the spin spiral plane and the structure exhibits just gradual transformation of the cone configuration to fully polarized state without intermediate phase transitions [1, 11]. We observed two kinds of the temperature evolution of the doublet ESR signals at cooling below T_N : i) At low frequencies ($\nu < 40$ GHz), the spinon doublet is gradually transformed into a single narrow line of the antiferromagnetic resonance, as shown in Fig. 3. ii) For higher frequencies, $\nu > 60$ GHz, the doublet found in the spin-liquid phase survives deep in the ordered phase, see Fig. 4. In the intermediate

frequency range $40 < \nu < 60$ GHz, there is a single ESR line, which is, however, strongly broadened with respect to observations in the low frequency range. Examples of the low temperature ESR lines at different frequencies are displayed on Fig. 5. The ESR lines, which arise via the temperature evolution of the first type, are marked here as ν_1 . Besides, there is a low-frequency branch of the ESR (marked as ν_2 on Figs. 5, 6), which was observed at the frequency 26.9 GHz and only in the ordered phase. The collection of resonance fields observed at $T < 0.1$ K in the whole frequency range is presented on the frequency-field diagram Fig. 6. Weak resonances, marked by "w" on Figs. 5, 6 were observed at several frequencies in the intermediate frequency range 40-60 GHz. In summary, for $\mathbf{H} \parallel a$, at $T < 0.1$ K we observe in the low frequency range narrow ESR lines corresponding to two branches - ν_1 , with a rising frequency-field dependence, and a low frequency branch ν_2 . In the high frequency range above 60 GHz there is a doublet of ESR lines analogous to that observed in the spin-liquid phase.

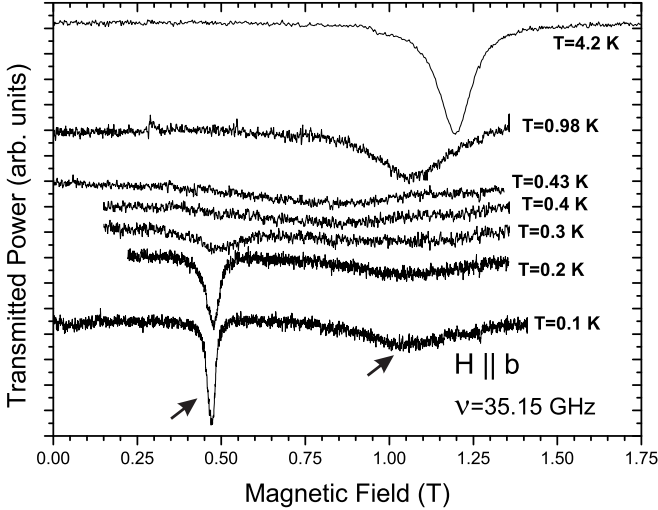


FIG. 7. Temperature evolution of the 35.15 GHz ESR signal at $\mathbf{H} \parallel b$.

Field along b-axis.

For $\mathbf{H} \parallel b$, there is a single ESR line in the spin-liquid phase. This resonance is shifting to lower fields with cooling. The shift of the resonance field from the magnetic field of the ESR of noninteracting spins $H_0 = 2\pi\hbar\nu/(g_b\mu_B)$ becomes visible at temperatures below 4 K. On further cooling, below the Néel temperature, the resonance line is strongly broadened near T_N and then reappears as a narrow line at $T \sim 0.3$ K, this evolution is illustrated in Fig. 7. Another resonance mode appears at low temperatures at higher field. These two modes are marked by arrows on Fig. 7. In the tem-

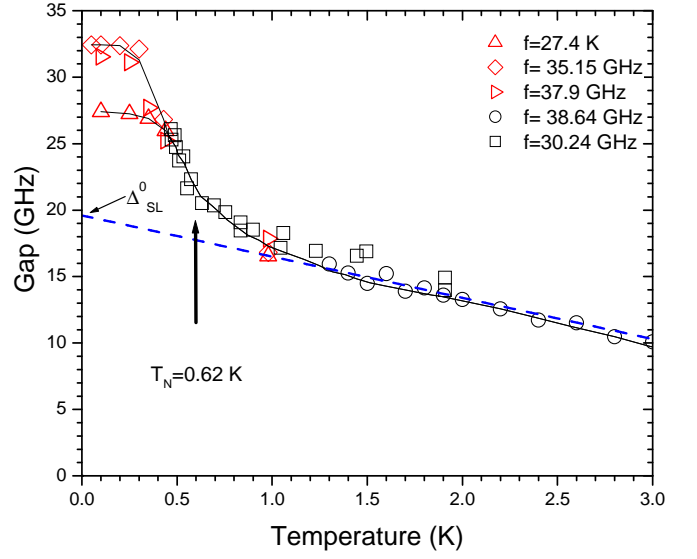


FIG. 8. Temperature dependence of the gap Δ , calculated from the equation (1) using the resonance field values at different frequencies for $\mathbf{H} \parallel b$ in the spin-liquid and ordered phases. Solid lines are guide to the eyes. Dashed line is the extrapolation of the spin-liquid energy gap to $T = 0$.

perature range of the spin-liquid state the value of the shifted resonance field may be described by the relation for a conventional gapped resonance (see Ref. [8]):

$$\nu^2 = \left(\frac{g_b\mu_B H}{2\pi\hbar}\right)^2 + \Delta^2 \quad (1)$$

The temperature dependence of the gap Δ , derived from the experiments on different frequencies, using the relation (1) is presented on Fig. 8. The gap is gradually rising on cooling from $T = 4$ K with a steep increase below T_N . In the ordered phase, below 0.4 K, we resolve two modes with different gaps, the resonance fields of both modes were used for calculation of the $\Delta(T)$ dependence presented on Fig. 8. The low-temperature limit of the lowest gap 28 GHz is twice as large as the gap at T_N . The low-field resonance on Fig. 7 corresponds to a branch with a rising frequency *vs* field dependence and has a narrow linewidth $\Delta H_s \sim 0.02$ T in the frequency range 35-43 GHz. These resonances are marked as ν_s on Fig. 9, where examples of ESR lines taken at different frequencies are presented. The resonances, observed at low temperature are collected on the frequency-field diagram Fig. 10. A family of low-frequency resonances with the frequencies below 35.5 GHz, including the upper field resonance of Fig. 7 is marked as ν_{lf} on Figs. 9, 10. At higher frequencies, 40-45 GHz, the resonance ν_s is superimposed with a broad line ν_b with a width of $\Delta H_b \sim 0.5$ T. In the range 45-50 GHz the broad line ν_b appears alone, and at higher frequencies the narrower line ν_{hf} with a width $\Delta H_{hf} \sim 0.2$ T is observed. Thus, the spectrum undergoes a crossover between the low fre-

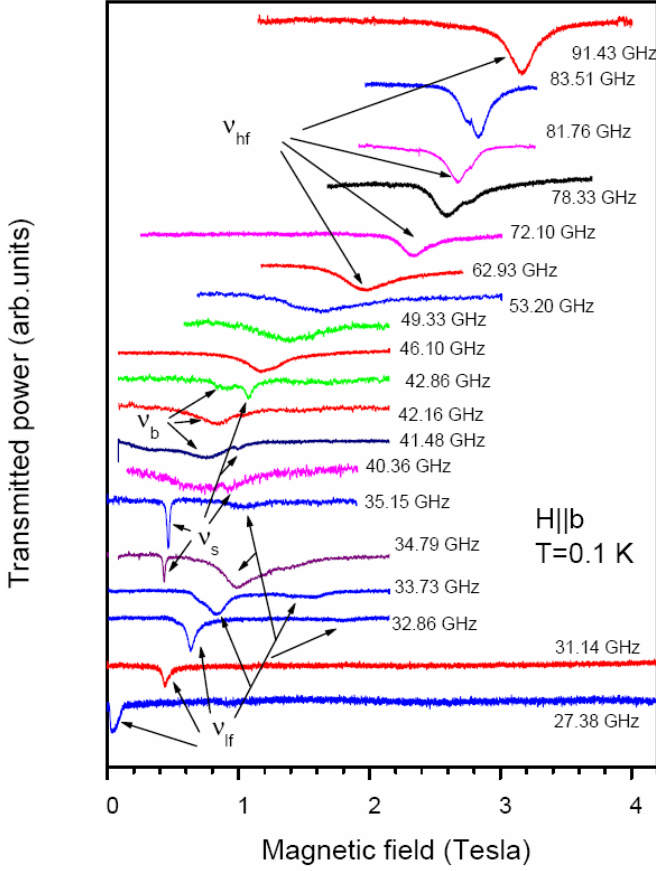


FIG. 9. Examples of low temperature ESR lines at $\mathbf{H} \parallel \mathbf{b}$, taken at different frequencies.

quency sharp resonance mode ν_s and the high frequency resonance ν_{hf} via coexisting resonances and a broad resonance in the intermediate frequency range $40 < \nu < 60$ GHz.

For the fields in the vicinity of 2.8 T we observe an abrupt modification of the ESR lines, which is clearly seen on Figs. 9, 11. This modification corresponds to a small step in the $\nu(H)$ dependence, presented on the insert of Fig. 10. The field $H = 2.8 \pm 0.05$ T of the step on the $\nu(H)$ dependence corresponds well to the field-induced phase transition at $H_{c1}^b = 2.75$ T observed in Ref. [11] as a jump on the magnetization curve.

Field along c -axis

For $\mathbf{H} \parallel \mathbf{c}$, a doublet of ESR lines appears in the spin liquid phase. At further cooling, as in the case of $\mathbf{H} \parallel \mathbf{a}$, for $\nu < 40$ GHz we observe the evolution to a single ESR line, while for $\nu > 60$ GHz the doublet survives at low temperatures, as presented in Fig. 12. Fig. 13 presents the temperature evolution of the resonance line till the lowest temperature $T < 0.1$ K, demonstrating the

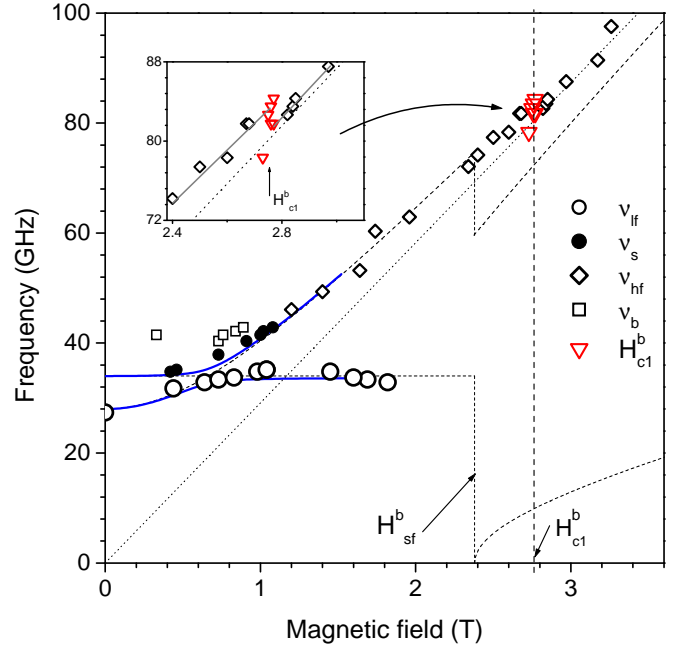


FIG. 10. Frequency-field diagram for $T=0.1$ K and $\mathbf{H} \parallel \mathbf{b}$. Triangles mark the field H_{c1}^b of the phase transition, measured on ESR records, other symbols represent resonances, marked in Fig.9. Dashed lines present the calculation according to the macroscopic theory for $\mathbf{H} \parallel \mathbf{b}$, solid lines - for 5° tilting angle between \mathbf{H} and \mathbf{b} . Dotted line is the paramagnetic resonance frequency for $g=2.08$. Field H_{sf}^b represents calculation by formula (9) of the Appendix. Vertical dashed line represent the field H_{c1}^b measured in Ref.[11]. Insert: frequency-field dependence in the vicinity of the phase transition.

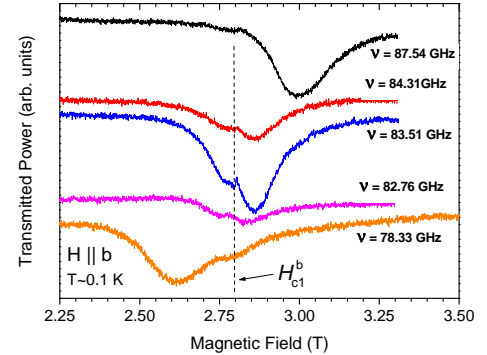


FIG. 11. ESR signals near the field-induced phase transition at $H_{c1}^b = 2.75$ T, $\mathbf{H} \parallel \mathbf{b}$.

evolution to the narrow line with the width $\Delta H = 0.04$ T. The resonance lines at different frequencies are given in Figs. 14, 15, the frequency-field diagram is presented on Fig. 16. At low temperature, in the low-field range we observe a strongly rising resonance branch, and a slowly falling one, marked as ν_1 and ν_2 correspondingly on Figs. 14, 16. In the low field range the ν_1 branch is observed as very narrow ($\Delta H_1 = 0.03$ - 0.04 T) resonance, while in

the frequency range above 50 GHz (corresponding to the field range 1.5-2.5 T) the resonance line is distorted, and at frequencies higher than 70 GHz there is again a doublet, analogous to the case of $\mathbf{H} \parallel a$. In the frequency range 37-64 GHz the ESR records have pronounced kink, which marks the value of the field of the phase transition at $H_{c1}^c = 1.48\text{ T}$, as illustrated on Fig. 17. The step on the frequency-field dependence at H_{c1}^c corresponds well to the phase transition observed by magnetization measurement at the same field as a step in magnetization and a jump in the susceptibility [11]. Besides, three low-frequency branches of lower intensities are detected in higher fields. Two of these branches are marked as $\nu_{e,g}$ on Figs. 14, 16. The third, high-field resonance mode, ν_h , is presented on Fig. 15, its frequency-field dependence is shown on Fig. 16. The resonances $\nu_{e,g}$ constitute a branch emerging above the field of the phase transition at $H_{c2}^c = 2.1\text{ T}$, also observed in Ref. [11]. The branch ν_h is observable in the field range between 7 and 8 T. This field range corresponds to a high-field phase, which was observed in Ref. [11] between the fields $H_{c4}^c = 7\text{ T}$ and $H_{sat} = 8\text{ T}$.

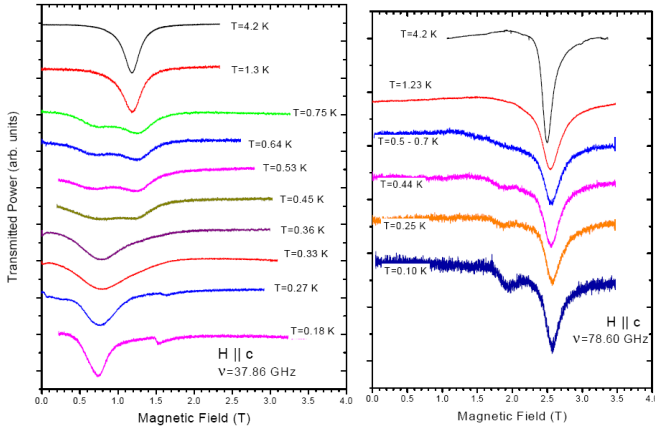


FIG. 12. ESR signals at $\mathbf{H} \parallel c$ for different temperatures.

DISCUSSION

The nature of the spin ordering in Cs_2CuCl_4 is a curious subject, because of the frustration of the lateral exchange bonds, causing the decoupling of spin chains. The ordered phases and field-induced transitions of Cs_2CuCl_4 are discussed in detail in Ref. [5]. At $H=0$, the ordering is supposed to be due to the joint action of the in-chain exchange J , the Dzyaloshinsky-Moriya interaction between ions on lateral bonds of triangular lattice (D'_a -term of Ref. [5]) and the frustrated exchange J' . This interplay should cause the "DM-spiral" with the spins lying in the bc -plane (see Ref. [5]), as confirmed by the experiment [1]. At the magnetic field $\mathbf{H} \parallel a$ the spiral ordering

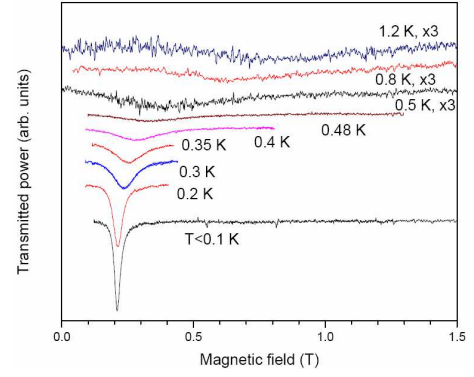


FIG. 13. ESR signals at $\mathbf{H} \parallel c$ for different temperatures at 34.5 GHz.

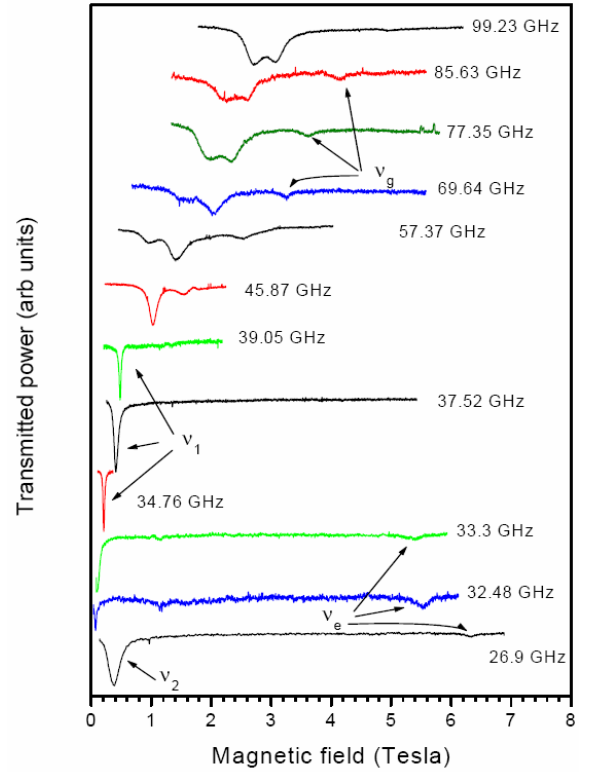


FIG. 14. ESR signals at different frequencies for $\mathbf{H} \parallel c$, $T < 0.1\text{ K}$

of transversal spin components takes place until the saturation field, as expected in theory and observed in experiment. However, at $\mathbf{H} \parallel b, c$ and $H \simeq D'_a$ the spin spiral is expected to flop perpendicular to the magnetic field and the above D'_a -term becomes ineffective for the flopped configuration. At $\mathbf{H} \parallel b$, the phase should be than ordered due to the action of J and J'' , resulting in the collinear AF phase. At $\mathbf{H} \parallel c$, another Dzyaloshinsky-Moriya term, D'_c becomes effective in the flopped phase and the most complicated sequence of phase transitions

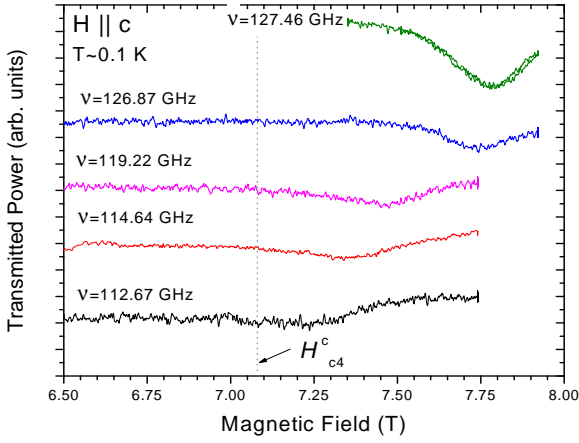


FIG. 15. ESR signals of the high-field mode ν_h . $\mathbf{H} \parallel c$, $T < 0.1$ K.

occurs. The spin structures for field-induced phases at $\mathbf{H} \parallel b, c$ are proposed in Ref. [5] by the consideration of the interactions characterized by the parameters $J, J', J'', D'_{a,c}$. The uniform Dzyaloshinsky-Moriya interaction, parametrised by $D_{a,c}$ terms does not contribute to the selection of the long range ordered ground states because its sign oscillates from one chain to another. According to the analysis of ordered phases [5], for $\mathbf{H} \parallel b$, two transitions before saturation are predicted, and for $\mathbf{H} \parallel c$ - four transitions before saturation. This corresponds well to the observations of Refs. [1, 11, 12], where the field-induced transitions are observed for $\mathbf{H} \parallel b$ in fields $H^b_{c1,2}$, and for $\mathbf{H} \parallel c$ in fields $H^c_{c1,2,3,4}$. These fields, except for H^b_{c2} are marked on Figs. 10, 16.

We interpret magnetic resonance in the ordered phase of Cs_2CuCl_4 in low fields, where the planar spin spiral is stable for all directions of the magnetic field. The antiferromagnetic resonance of a planar spiral structure with two axes of the anisotropy should obey two gapped modes of the antiferromagnetic resonance and a zero-frequency Goldstone mode, see, e.g. Ref. [13]. Two modes with different gaps correspond to out of plane oscillation of the spiral spin system and the third mode with a zero frequency represents in-plane rotation of the spiral which may be performed without the energy loss. The low-frequency dynamics of the planar spiral antiferromagnet was described in Ref. [13] using the macroscopic approach developed in Ref. [14]. In this approach one considers the spiral spin structure parametrised by two orthogonal unit vectors \mathbf{l}_1 and \mathbf{l}_2 :

$$\mathbf{S} = \mathbf{l}_1 \sin(\mathbf{q}\mathbf{r}) + \mathbf{l}_2 \cos(\mathbf{q}\mathbf{r}) \quad (2)$$

The consideration is valid in the exchange approximation, i.e. in the magnetic fields far below the saturation ($H_{sat} \simeq 8$ T for Cs_2CuCl_4) and for low frequency $2\pi\hbar\nu \ll J$, it does not involve the resonance absorption due to the transitions of magnons over a gap at

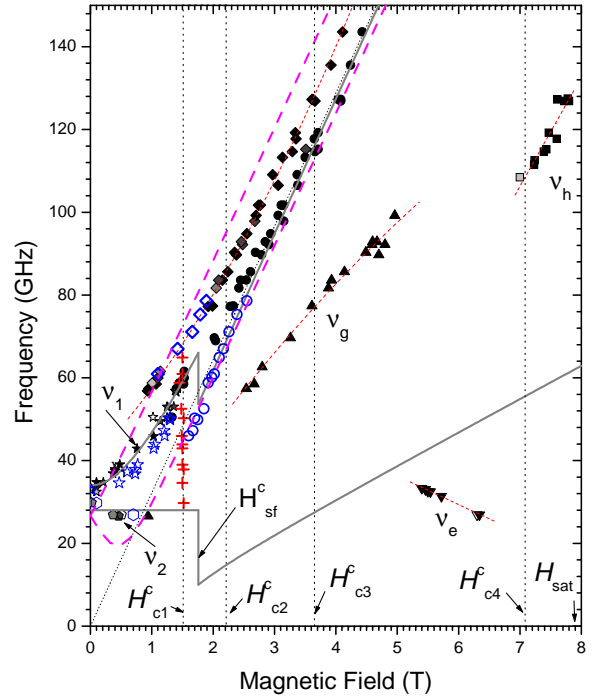


FIG. 16. frequency-field dependence for ESR signals at $\mathbf{H} \parallel c$. Filled and empty symbols correspond to two different samples, crosses - to values of H^c_{c1} , measured as kinks on ESR records at different frequencies. Solid grey lines present macroscopic theory, thin dashed lines are guide to eyes, thick dashed lines present the proposed spinon-type resonances ν_{\pm} , according to relation (3). Dotted line presents the high-temperature ESR. Vertical dashed lines correspond to critical fields $H^c_{c1,2,3,4}$, observed in magnetization experiments in Ref. [11]. The saturation field H_{sat} is marked according to ref. [11]. The field H^c_{sf} presents the calculated spin-flop field according to formula (10).

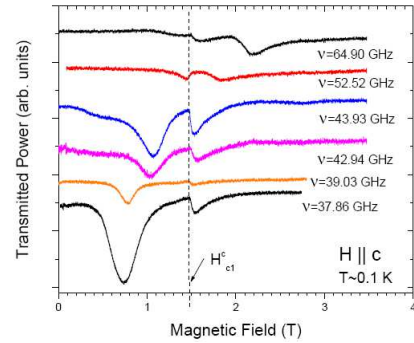


FIG. 17. ESR signals at $\mathbf{H} \parallel c$ near the field induced transition. H^c_{c1} is marked according to Ref.[11].

the wavevector of the spiral. The resonance frequencies obtained by this approach are represented in Sec. Appendix, equations (6-8). This consideration predicts also spin-flop transitions for $\mathbf{H} \parallel b, c$ in the magnetic fields $H^{b,c}_{sf}$ given by (9,10). At these fields the spin plane should flop perpendicular to the magnetic field because

of the anisotropy of the susceptibility.

The experimental frequencies for all three directions of the magnetic field were fitted by the relations (6-8) in the low field range. The exchange approximation does not involve the anisotropy of g -factor. We include the anisotropy of g -factor by taking the value of $\gamma = g_{a,b,c}\mu_B/\hbar$ for orientations of \mathbf{H} along the axes a, b, c correspondingly. The frequency-field dependences, calculated for $\mathbf{H} \parallel a, c$ are presented on Figs. 6, 16 by solid lines. For the orientation $\mathbf{H} \parallel b$ the intersection of calculated branches takes place. This causes a repulsion of branches in case of a tilting of the magnetic field with respect to the b -axis. The frequency, calculated for a perfect $\mathbf{H} \parallel b$ orientation is presented on Fig. 10 by dashed line, while $\nu(H)$, modeled for the tilting angle of 5° is given by a solid line. Calculated curves for both perfect and tilted configurations agree with the experimental resonance frequencies, while the calculation for the tilted field gives a better coincidence with the evolution of the resonance field at a gradual increase of the frequency.

The fitting parameters are $\omega_{10}/(2\pi) = 34 \pm 2$ GHz and $\omega_{20}/(2\pi) = 28 \pm 2$ GHz, $A = -7.2 \cdot 10^6$ erg/mole $= -8.6 \cdot 10^{-2}$ K/Cu and $B = -2.3$ erg/mole $= -2.7 \cdot 10^{-3}$ K/Cu. The energy of the anisotropy, presented by constants A and B are much smaller than the main exchange integral $J = 4.3$ K and the constant of uniform Dzyaloshinsky-Moriya interaction derived in Ref. [8] $D = 0.4$ K. The constant of the staggered Dzyaloshinsky-Moriya interaction, derived from neutron scattering experiments in polarised state is $D'_a = 0.23$ K. Parameter η was calculated using the susceptibility values measured in Ref.[11]: $\chi_{\parallel} = 4.9 \cdot 10^{-2}$ and $\chi_{\perp} = 3.7 \cdot 10^{-2}$ emu/mole for $T \rightarrow 0$. It is worth to note that the parameter η , calculated in such a way, does not correspond exactly to the parameter of the anisotropy of the susceptibility considered in the theory of Ref. [13], because the anisotropy of the susceptibility is of the same order as that of the g -factor, while the theoretical model considers parameter η in the exchange approximation with an isotropic g -factor. Besides, the condition of the low frequency approximation $\hbar\omega \ll J$ is not valid for the case of Cs_2CuCl_4 , because observed gaps (~ 30 GHz) are about a half of $J/(2\pi\hbar)$. Due to violation of conditions of applicability and above cited approximations, we consider the results given in the Appendix as providing only a qualitative description and classification of modes of antiferromagnetic resonance and giving the approximate values of spin-flop transitions for Cs_2CuCl_4 . In particular, the absence of a good correspondence between the calculated spin flop fields $H_{sf}^{b,c}$ and the observed values $H_{c1}^{b,c}$ is attributed to these approximations. The values of observed [11] field-induced transitions and of the calculated spin-flop fields are marked on Figs. 10,16.

Thus, the experiment in the lower range, $\nu < 40$ GHz, corresponds qualitatively to the macroscopic approach

(6-8). However, increasing the frequency to a value of the order of the exchange frequency $J/(2\pi\hbar) = 67$ GHz and higher, we observe at $\mathbf{H} \parallel a, c$ a gradual transformation of the upper branch of the antiferromagnetic resonance ν_1 into a doublet of lines. A transformation of ESR line is also observed for the third orientation, $\mathbf{H} \parallel b$, there is an evolution of a narrow ESR line to a broadened one via an intermediate resonance at $40 \text{ GHz} < \nu < 50 \text{ GHz}$. Therefore, the spectrum observed in the high frequency range, is analogous to that in the spin-liquid phase, i.e. a doublet for $\mathbf{H} \parallel a, c$ and a single gapped line for $\mathbf{H} \parallel b$.

To check this, we suggest to extrapolate the hypothetical spinon-type doublet ESR frequencies ν_{\pm} with the spin-liquid ansatz based on equations (4,5) of Ref. [8]. Specifically, we attempt to describe resonance frequencies of the doublet with the relation

$$\nu_{\pm} = \nu_{R,L} + \delta\nu, \quad (3)$$

where $\nu_{R,L}$ are taken from (4,5) of Ref. [8] but with extrapolated values $D_a = 10.4$ GHz and $D_c = 14.3$ GHz which have been increased by 30% from their measured at $T = 1.3$ K values. This correction should be made because the gap induced by Dzyaloshinsky-Moriya interaction, $\Delta = \frac{\pi}{2}\sqrt{D_a^2 + D_c^2}$, measured in the spin liquid phase above T_N is observed to slowly increase with lowering of the temperature, see Fig. 8. This suggests, that the zero-temperature values of D_a and D_c are larger, than values extracted from $T = 1.3$ K measurements. Of course, these parameters cannot be measured directly at low temperature, where the inter-chain exchange and other residual interactions establish the three-dimensional long range order. The ordering produces a steep increase of the gap in the neighborhood of $T_N = 0.62$ K, see Fig. 8. Nevertheless, we can estimate the $T = 0$ "spin-liquid gap" extrapolating the temperature dependence of Δ in Fig. 8 from the spin-liquid range. Linear extrapolation of $\Delta(T)$, shown by the dashed line on Fig. 8, results in $\Delta_{SL}^0 = 19.6$ GHz, and represents a 30 % increase of $D_{a,c}$ from their $T = 1.3$ K values when $\Delta = 15$ GHz. The second term in eq. (3), $\delta\nu = \frac{\omega_{20}}{2\pi} - \Delta_{SL}^0 = 9$ GHz is an empiric way to account for the renormalization of the gap by the three dimensional magnetic ordering. The values of ν_{\pm} calculated in this way are shown by thick dashed lines on Figs. 6, 16. We see that the high-frequency experimental data correspond well to this quasi-empirical proposition for $\mathbf{H} \parallel a$ and there is a qualitative correspondence for $\mathbf{H} \parallel c$, i.e. the splitting of the doublet observed in the ordered phase has a natural value for the spin liquid state extrapolated to zero temperature. Thereby, the changes in the ESR lineshape and spectrum observed at increasing the frequency for all three principal orientations $\mathbf{H} \parallel a, b, c$ mark a crossover from antiferromagnetic resonance to a spinon type ESR. In addition, following the temperature evolution of ESR (Figs. 4, 12) from the spin liquid to the

ordered phase we also can interpret the doublet observed in the high frequency range $\nu > 60$ GHz at $\mathbf{H} \parallel a, c$ as the spinon type ESR formed in the spin-liquid phase and surviving deep in the ordered phase.

Thus, if the magnetic field is large enough, i.e. $\mu_B H \simeq J$, we may conclude, that the two spinon continuum near $q \simeq 0$ remains unchanged in the ordering process and further cooling. At lower fields (and lower frequencies $\nu < J/(2\pi\hbar)$), for $q=0$, the continuum is replaced by antiferromagnetic resonance of the ordered spiral structure. The spectrum with the coexistence of the spinon type ESR and of the antiferromagnetic resonance indicates a new kind of magnetic resonance, arising due to the specific ground state with the ordered spin components and strong zero point fluctuations. As far we know, there is no adequate theory for this type of ESR.

The observation of the coexistence of two kinds of ESR signals in the ordered phase of Cs_2CuCl_4 is naturally related to a similar feature of the inelastic neutron scattering experiments of Ref. [2]. In these (zero-field) experiments, at cooling below T_N , the spinon continuum was found to remain practically unchanged for the energy range above 0.2 meV (i.e 50 GHz), while in the narrow interval near the lowest boundary a spin wave mode at 0.1 meV (25 GHz) was found below T_N , see Fig. 6 of Ref. [2]. In our experiments we observe that the spinon-type ESR remains approximately undistorted at high frequency, while it is replaced by the antiferromagnetic resonance at low frequency. We can not still interpret the weak modes $\nu_{e,g,h}$, observed for field-induced phases at $\mathbf{H} \parallel \mathbf{c}$ because the spin structure for these phases is formed under a complex interplay of several interactions.

CONCLUSION

The electron spin resonance, corresponding to a two spinon continuum of quantum critical $S = 1/2$ spin chain was found to exist both above and below the ordering point T_N in the frequency range above the exchange frequency $J/(2\pi\hbar)$. At the same time, in the low frequency range, the spinon type ESR is replaced by the antiferromagnetic resonance below the Néel point.

ACKNOWLEDGEMENTS

Authors acknowledge K. O. Keshishev for guidance in use of the dilution refrigerator and O. A. Sarykh, S.S. Sosin, for useful discussions. The work was supported by Russian Foundation for Basic Research, grants 11-02-12225 and 12-02-00557.

APPENDIX

The Lagrange function of a mole of a planar spiral magnet is

$$\mathcal{L} = \frac{\chi_{\parallel}(1-\eta)}{4\gamma^2}((\dot{\mathbf{l}}_1 + \gamma[\mathbf{l}_1 \times \mathbf{H}])^2 + (\dot{\mathbf{l}}_2 + \gamma[\mathbf{l}_1 \times \mathbf{H}])^2) + \frac{\chi_{\parallel}(1+\eta)}{4\gamma^2}(\dot{\mathbf{n}} + \gamma[\mathbf{n} \times \mathbf{H}])^2 - U_a \quad (4)$$

Here $\mathbf{n} = [\mathbf{l}_1 \times \mathbf{l}_2]$ and $\eta = 1 - \frac{\chi_{\perp}}{\chi_{\parallel}}$, χ_{\parallel} is the susceptibility along \mathbf{n} , and χ_{\perp} - is the susceptibility in the spin plane. $\gamma = \mu_B/\hbar$ is the gyromagnetic ratio for the spin angular momentum. The energy of magnetic anisotropy may be taken in the quadratic form as

$$U_a = \frac{1}{2}(An_z^2 + Bn_y^2) \quad (5)$$

Taking the axes as follows $a \rightarrow z \parallel \mathbf{n}$, $b \rightarrow x$, $c \rightarrow y$, with $A < 0$, $A < B$, we have in the ground state a spiral within the bc plane. Varying the Lagrangian (4) with respect to $\delta \mathbf{l}_1$, $\delta \mathbf{l}_2$ we get the resonance frequencies.

1) for $\mathbf{H} \parallel b$

$$\omega = \omega_{10}, \sqrt{\omega_{20}^2 + (\gamma H)^2} \quad (6)$$

2) $\mathbf{H} \parallel c$

$$\omega = \omega_{20}, \sqrt{\omega_{10}^2 + (\gamma H)^2} \quad (7)$$

3) $\mathbf{H} \parallel a$

$$\omega^2 = \frac{\omega_{10}^2 + \omega_{20}^2}{2} + (\gamma H)^2 \frac{2 + \eta^2}{4} \pm \left(\frac{(\omega_{10}^2 - \omega_{20}^2)^2}{4} + 2(\gamma H)^2(\omega_{10}^2 + \omega_{20}^2) \frac{(1 + \eta)^2}{4} + 4(\gamma H)^4 \frac{(1 - \eta^2)^2}{16} \right)^{1/2} \quad (8)$$

$$\text{Here } \omega_{10}^2 = \frac{-A}{\chi_{\parallel}}\gamma^2, \omega_{20}^2 = \frac{B-A}{\chi_{\parallel}}\gamma^2.$$

For $\chi_{\parallel} > \chi_{\perp}$ there should be a spin flop transition at the in-plane magnetic fields H_{sf} , at which the spin plane flops perpendicular to the magnetic field. These critical fields may be calculated in the same low-field approximation for the magnetic field along b and c correspondingly:

$$H_{sf}^b = \frac{\omega_{10}}{\gamma\sqrt{\eta}} \quad (9)$$

$$H_{sf}^c = \frac{\omega_{20}}{\gamma\sqrt{\eta}} \quad (10)$$

For $H \parallel b$ the resonance frequencies at $H > H_{sf}^b$ should be calculated by formula (8), with $\omega_{10}^2 = \frac{A}{\chi_{\parallel}}\gamma^2$ $\omega_{20}^2 = \frac{B}{\chi_{\parallel}}\gamma^2$.

For $H \parallel c$ at $H > H_{sf}^c$, the resonance frequencies should be calculated by (8) with

$$\omega_{10}^2 = -\frac{B}{\chi_{\parallel}}\gamma^2 \text{ and } \omega_{20}^2 = \frac{A-B}{\chi_{\parallel}}\gamma^2.$$

REFERENCES

-
- [1] R. Coldea, D. A. Tennant, A. M. Tsvelik, Z. Tylchynski, Phys. Rev. Lett. **86**, 1335 (2001).
 - [2] R. Coldea, D. A. Tennant, Z. Tylczynski Phys. Rev. B **68**, 134424 (2003).
 - [3] M. Kohno, O. A. Starykh, and L. Balents, Nat. Phys. **3**, 790 (2007).
 - [4] D. Heidarian, S. Sorella, F. Becca, Phys. Rev. B **80**, 012404 (2009).
 - [5] O. A. Starykh, H. Katsura, L. Balents, Phys. Rev. B **82**, 014421 (2010).
 - [6] R. Coldea, D. A. Tennant, R. A. Cowley, D. F. McMorrow, B. Dorner and Z. Tylczynski, J. Phys. Condens. Matter **8**, 7473 (1996).
 - [7] S. Gangadharaiah, J. Sun, O. A. Starykh, Phys. Rev. B **78**, 054436 (2008).
 - [8] K. Yu. Povarov, A. I. Smirnov, O. A. Starykh, S. V. Petrov and A. Ya. Shapiro, Phys. Rev. Lett. **107**, 037204 (2011).
 - [9] H. Karimi and I. Affleck, Phys. Rev. B **84**, 174420 (2011).
 - [10] T. Sakon, H. Nojiri, K. Koyama, T. Asano, Y. Ajiro and M. Motokawa, J. Phys. Soc. Japn. 72 Suppl.B, 140 (2003).
 - [11] Y. Tokiwa, T. Radu, R. Coldea, H. Wilhelm, Z. Tylczynski, F. Steglich, Phys. Rev. B **73**, 134414 (2006).
 - [12] M. Takigawa NMR experiment, private communication
 - [13] L. E. Svistov, L. A. Prozorova, A. M. Farutin, A. A. Gippius, K. S. Okhotnikov, A. A. Bush, K. E. Kamentsev, and E. A. Tischenko Zh. Eksp. Teor. Fiz. **135**, 1151 (2009) [JETP **108**, 1000 (2009)].
 - [14] A.F. Andreev, V.I. Marchenko. Sov. Phys. Uspekhi 23, 21 (1980)